

# A new numerical approach to find current distribution and AC losses in coaxial assembly of twisted HTS tapes in single layer arrangement

Majid Siahtrang<sup>1</sup>, Frédéric Sirois<sup>1</sup>, Francesco Grilli<sup>2</sup>, Slobodan Babic<sup>1</sup> and Simon Brault<sup>1</sup>

<sup>1</sup> École Polytechnique de Montréal, Montréal, QC, H3C 3A7, Canada

<sup>2</sup> Forschungszentrum Karlsruhe GmbH, Hermann-von-Helmholtz-Platz 1, D-76344 Eggenstein-Leopoldshafen, Germany

E-mail: majid.siahtrang@polymtl.ca

**Abstract.** This paper presents a novel technique for evaluating AC losses and current distribution in single layer assemblies of coaxially wound thin conductors, such as YBCO coated conductors. The proposed approach takes into account the twisted geometry of the individual superconducting tapes by considering the integral relation between the magnetic vector potential and the current density in the tapes (Biot-Savart formula). The integrals are solved numerically and semi-analytically, and the results are used to generate a discretized system of equations based on the magnetic flux diffusion equation (eddy current problem). The latter is solved using an efficient time transient solver (DASPK). It is assumed that, due to the helical symmetry of the problem, it is sufficient to solve for the current distribution in half of a single tape cross-section, even if many tapes are present, which allows a drastic reduction of the 3-D problem to a simple 1-D domain. The method was used to evaluate the AC losses of a HTS cable made of coated conductors, and it was observed that for a given radius of the former and number of tapes, twisted tapes with smaller pitch have lower AC losses.

## 1. Introduction

Numerical computation of AC losses is an important technical issue for commercial application of second generation high-temperature superconductor (HTS) cables and it has been the subject of numerous research works in the area of applied superconductivity. In addition to the strongly nonlinear resistivity inherent to HTS materials, the complex geometry of the cable (involving twisted tapes with very high aspect ratio assembled in multi-layer arrangement) adds more difficulties to the accurate computation of AC losses<sup>1</sup>.

In order to make the problem easier to solve, the numerical techniques used to investigate the behavior of HTS cables usually do not take into account the real geometry. Several 2D methods neglecting the twisted configuration have been proposed for computing AC losses in HTS cables [1-4]. While providing useful information on the AC losses, these methods cannot be used for designing purposes, where finding the optimal twist design is an important issue.

<sup>1</sup> The paper investigates the behavior of coated conductor HTS cables. For sake of simplicity, in the paper we use the term “HTS cable” to refer to cables made of coated conductor.

Other methods simulating the cable as a HTS cylinder and using an anisotropic conductivity to take the twist into account have been developed, both with FEM (finite-element method) and non-FEM techniques [5, 6]. Although the twisted geometry is considered by these methods, the tape-to-tape gaps in each layer are omitted; it has been reported that this approximation leads to an underestimation of the AC losses [5].

In this paper, we propose a new and efficient technique for computing AC losses and current distribution in HTS cables. The technique is based on the formulation of the eddy current equation, it uses the integral relationship between current density and vector potential, and can directly take into account twisted geometries.

The paper is organized as follows. Firstly, we describe the mathematical formulation of the method; secondly, we compare the results with those obtained with a FEM model for the case of straight tapes; then we apply the method to the case of single-layer HTS cable with twisted tapes and we discuss the influence of the twist pitch on the current distribution and AC losses; finally, we summarize our results in the conclusion.

## 2. Numerical Method

The model proposed in this paper, which we call IM (Integral Method) hereafter, is based on the solution of eddy current equations discretized over a proper study domain in a 2D cross section of the cable. With this formulation, the state variable, current density  $J$  is related to the magnetic vector potential  $A$  by means of Biot-Savart law. Due to the use of this integral relation and the absence of any magnetic material, the study domain of the problem is confined to the current carrying superconducting layer of the tapes. This drastically decreases the number of degrees of freedom (DOF) of the problem compared to FEM simulations, where the area surrounding the tapes has to be considered and meshed. As a consequence, our method is more efficient in terms of memory requirements and computation time than classical FEM methods.

For sufficiently long cables, due to the symmetry of the helically wound tapes, knowing the current distribution over any 2D cross section of the cable is sufficient to accurately determine the AC losses. In addition, if the tapes are assembled in a symmetrical arrangement around the circumference of the former cylinder (as is the case of HTS cables), the study domain can be reduced to half of one tape. Finally, due to the high aspect ratio of the superconducting layer of the YBCO tapes, the study domain can be even more reduced and assimilated to a 1D straight line. These study domain reduction steps, from the real 3D geometry to a straight discretized line are shown in figure 1.

Once the study domain is established in the form of finite interconnected straight lines (figure 1d), the eddy current equation is formulated for each element  $i$  as  $E_i = -\partial A_i / \partial t - \nabla V$ , where  $E$  and  $A$  are the electric field and the magnetic vector potential, respectively.  $\nabla V$  represents the potential gradient, which is constant over the tape cross-section. Using  $E = \rho J$  as constitutive equation, the electric field is substituted with a function of the current density. In the case of HTS tapes, the power-law model  $\rho = E_c / J_c |J / J_c|^{n-1}$  was used to define the nonlinear resistivity of the HTS material. Based on the symmetry arguments specific to this kind of geometry, it is intuitive that the current flowing inside the tapes can not deviate from the helical path along which the tapes are wound. Therefore, the current density (which is assumed to be constant within each elements) is aligned with the helical trajectory of the tapes. The relation between  $J$  and  $A$  is addressed by introducing an  $k$  by  $k$  matrix as  $[A]_{k \times 1} = [M]_{k \times k} [J]_{k \times 1}$ , where  $k$  is the number of discretized elements, which determines number of DOFs of the problem.

Although the governing equation of the problem is formulated over a reduced 1D study domain, the exact 3D twisted geometry of each individual tape is taken into account to establish the  $M$  matrix. Each entry of  $M$  is obtained from the solution of the 3D Biot-Savart potential integral applied to helically wound strips. The width of each elementary strip is  $2 \times k$  times smaller than the width of an individual tape and carries a sheet current density of 1 A/m.

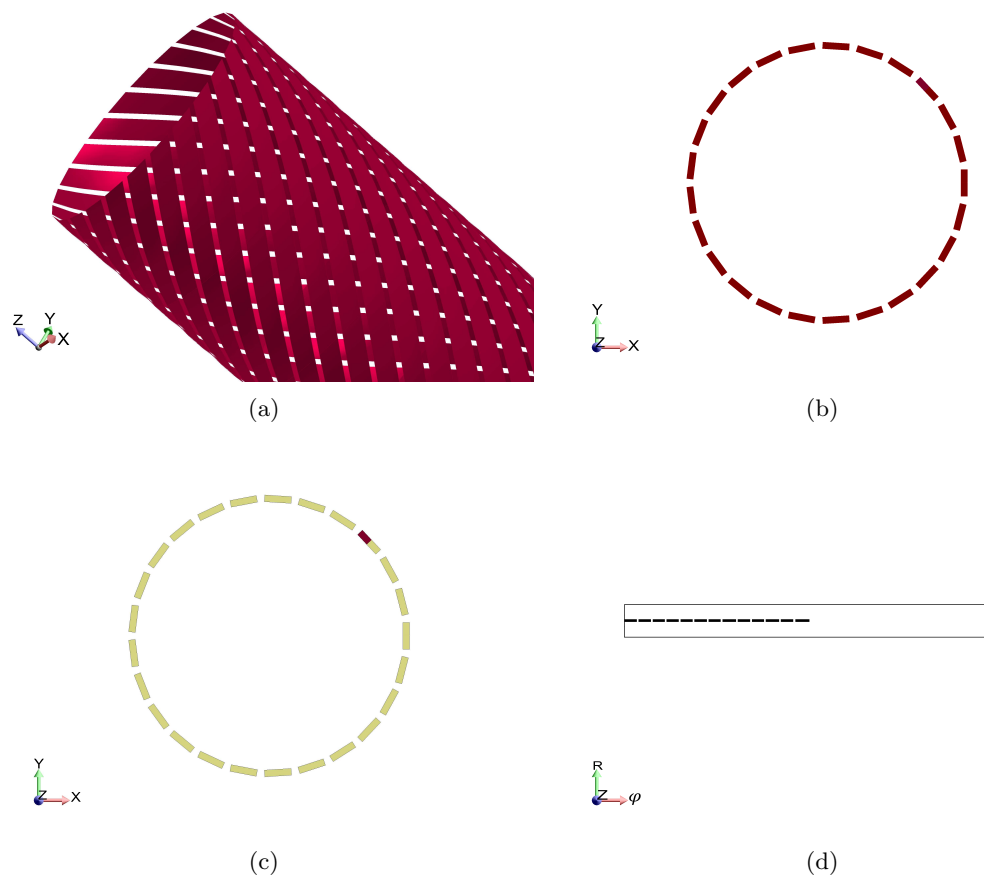


**Figure 1.** Successive reduction of study domain in the proposed hypothesis (tapes dimensions not drawn to scale). (a) Real 3D geometry, (b) 2D cross-section of the tapes, (c) Reduction of study domain to half of a tape, (d) Final study domain in the form of discretized interconnected 1D strips (straight lines) along half width of one tape.

As mentioned earlier, the magnetic solution for  $A$  is obtained by solving the Biot-Savart integral. Like all Biot-Savart type integrations, the denominator of the integrand tends towards zero when both the source and field points are the same or are located very close to each other. This will lead to inaccurate results at these singular or near singular points if using direct numerical integration. Since computation of  $A$  in these singular points will determine the diagonal entries of the  $M$  matrix, this inaccuracy is not acceptable here.

In order to get rid of the singularity problem, we proposed an alternative semi-analytic solution to solve the Biot-Savart integration for helically wound tapes. In this approach each tape is discretized along its longitudinal helical path while being discretized along its width. Then each obtained element is approximated with a rectangular infinitely thin sheet. In other words, each tape is approximated by a series of tiny interconnected rectangular elements. Thanks to the indefinite integration tools of the *Mathematica* software, the analytical solution of the Biot-Savart integral for such a rectangular element can easily be obtained. In the semi-analytic approach, this analytical solution will be used to find  $A$  at desired observation points by superposition of the contribution of all the elements. Since an analytic expression is used as the kernel of this method, therefore no singularities will be encountered even if the observation points are located within the tapes.

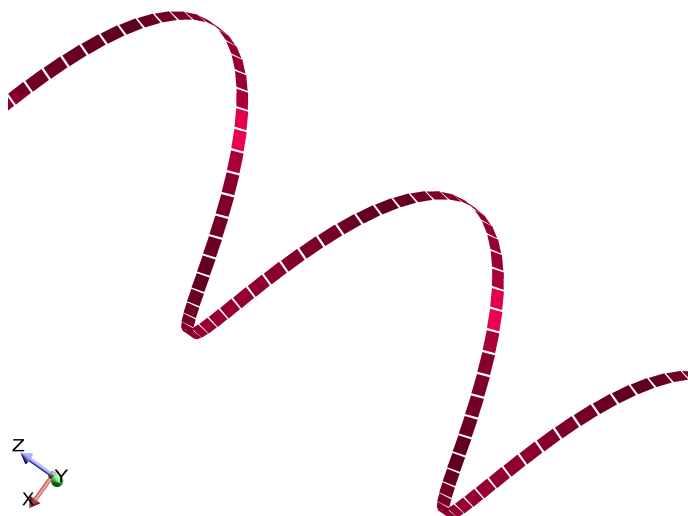


**Figure 2.** A twisted tape constructed by interconnecting many finite rectangular elements.

To set up the  $M$  matrix, a combination of both numerical integration and this semi-analytic approach was used. The semi-analytic method, which is more accurate at singular or near singular points, is used to consider the contribution of the parts of the tapes that are close to the observation points. An adaptive numerical integration, which is faster, was employed to model the remaining portion of the tapes. To model a long cable, this integration has to be done over a long enough length of the tapes. More details about both of these methods will be provided in a forthcoming publication.

Once the governing equations of the problem are formulated in their discretized version, an adaptive time transient solver with a sophisticated error estimator is used to solve it. One of these algorithms, called DASPK was already used in our previous works [7, 8], and is used here to solve the obtained system of differential algebraic equations(DAE). Finally, after  $J(t)$  is known in all the elements, AC losses are computed using the following formula

$$Q = 2fN \times \int \rho J^2 dl \quad (1)$$

where  $N$  denotes the number of tapes and  $f$  is the frequency of the transport current. This integration has to be carried out over the length of the study domain (half width of one tape).

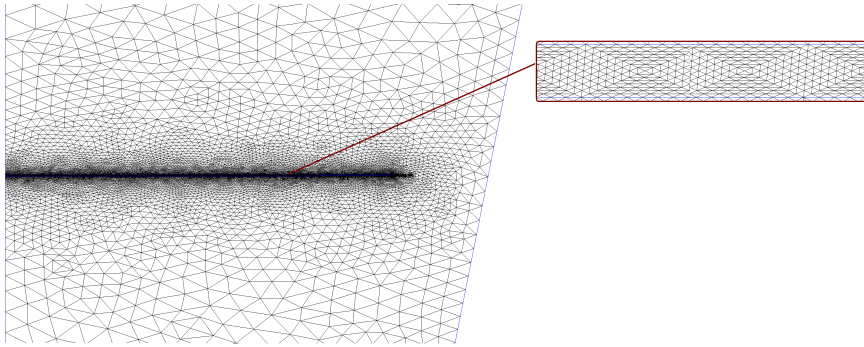
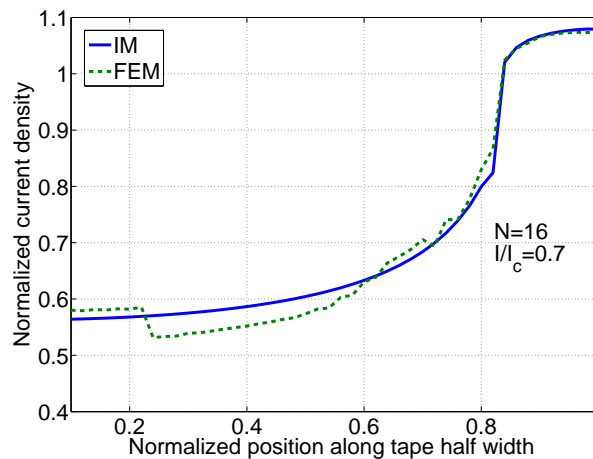
### 3. Validation methodology

Since at the present time we do not have access to experimental loss data for a single-layer HTS cable, nor have we developed a fully 3D FEM model for twisted tapes, we limited the validation of our model to the case of straight tapes. Therefore, in particular, we performed a 2D FEM simulation and computed the current distribution and the AC losses in an infinitely long cable with a former radius of 12.62 mm and composed of 16 straight tapes. For the FEM simulations, we used the edge-element model described in [9]. The tape parameters are listed in table 1. In the FEM simulations, a thickness of  $5 \mu\text{m}$  (instead of  $1 \mu\text{m}$ ) was used, in order to keep the number of DOFs at an acceptable level.

The transport current is 70% of the critical current and the frequency is 50 Hz. Considering a large value for pitch length, we launched the IM model to solve the same problem. The meshed FEM study domain is shown in figure 2. The number of DOFs in FEM simulation was 122935, against 50 only with the IM. As mentioned earlier, the large number of DOFs in the FEM model comes from the necessity of meshing a tape with a very high aspect ratio as well as the surrounding air region.

**Table 1.** Cable and tape properties.

Tape width	4 mm
Tape thickness	1 $\mu\text{m}$
Former radius	12.7 mm
N (number of tapes)	1 to 16
$J_c$	$10^{10}$ A/m <sup>2</sup>
n (power-law index)	25
Frequency	50 Hz

**Figure 3.** Meshed study domain in FEM simulation.**Figure 4.** Current density distribution along the tape width for a transport current amplitude of  $0.7I_c$  and  $N=16$  straight tapes, computed with IM and FEM.

The AC loss value computed by IM model is just 2.5% smaller than that computed by FEM. Also the computed current density distributions are very similar, as displayed in figure 4. Note that FEM simulation took more than 3 days to be solved while overall computation time of IM (included the  $M$  matrix generation) was less than an hour.

In addition, we applied the IM model to find the current distribution inside the tape in one of the cases simulated in [3] ( $N=8$  and tape width=10 mm), and we got exactly the same results (not shown here).

#### 4. Application of the IM to analysis of single layer twisted tapes

Since the twisted geometry of each individual tape is taken into account in the integral method proposed here, it can be applied to precisely determine the electrical performance of a single-layer arrangement of coaxially wound twisted tapes. Many geometrical parameters can be varied: in our simulations we kept the former radius fixed (12.7 mm), and we varied the number of tapes and the pitch length.

For different pitch lengths figure 5 presents the computed AC losses in each constituting tape per unit length of the cable as a function of  $N$  for a transport current equal to 70% of  $I_c$ . As expected, the AC losses decrease as the number of tapes increases. This is due to the fact that when the number of tapes increases the gap between the tapes decreases and for smaller gaps each tape experiences a magnetic field which is predominantly parallel to its width, whereas the perpendicular component near its edges tends to be smaller. The same observation has been reported in previous studies [2, 3].

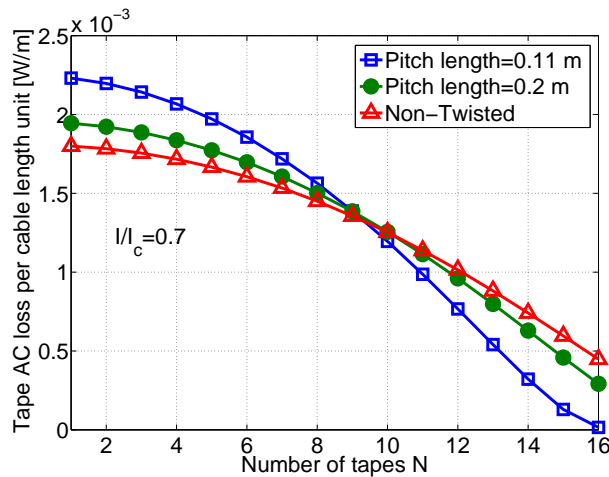


**Figure 5.** AC losses of a tape per cable length unit as a function of the number of tapes for different pitch lengths.

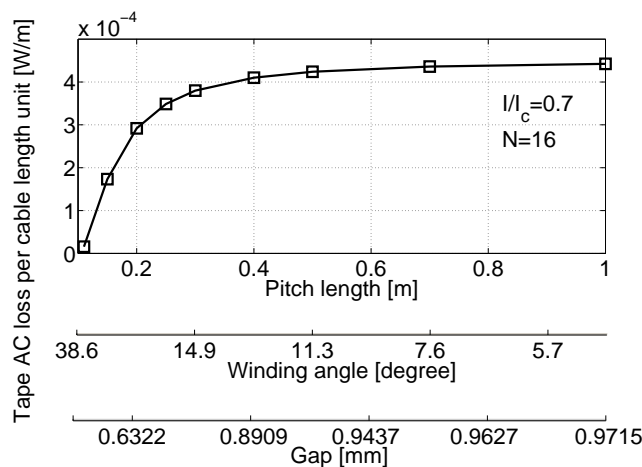


**Figure 6.** AC losses of a tape per cable length unit as a function of the twist pitch length.

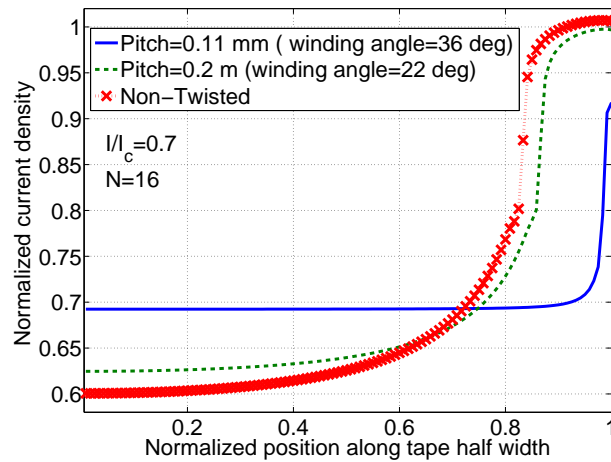


**Figure 7.** Current density distribution along the tape width for different twist pitch lengths.

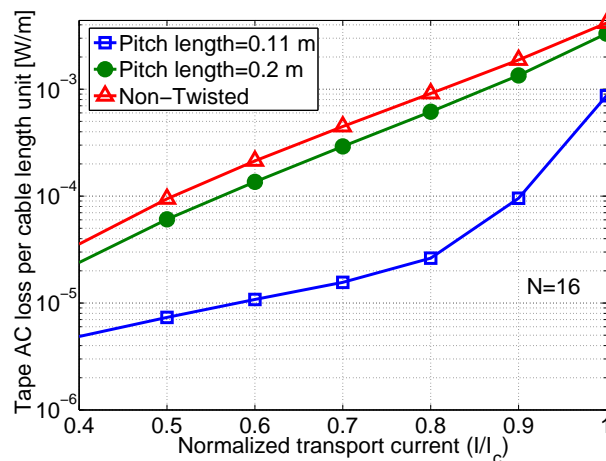


**Figure 8.** AC losses of a tape per cable length unit as a function of the transport current for different twist pitch lengths.

Since the former radius is fixed, for a given number of tapes  $N$  a smaller pitch length (i.e. a larger winding angle) results in a smaller tape-to-tape gap, which tends to reduce the losses, as discussed above. On the other hand, however, a smaller pitch length implies a longer tape per cable length unit, which ultimately results in higher losses. With figure 5 as reference, the following is observed:

- For  $N$  smaller than 9 tapes the tape-to-tape gap is large, so that the cancellation of most of the perpendicular field component at the tape's edge is not very effective; in this case the effect of a longer tape per cable length unit is dominant and the shorter the pitch length the higher the losses.
- For  $N$  greater than 9 tapes the tape-to-tape gap is small, the cancellation of the perpendicular field component is more effective and the consequent AC loss reduction is more important; in this case the shorter the pitch length the smaller the losses, because the loss reduction caused by placing the tapes closer to each other is more significant than the

loss increase caused by using a shorter pitch length.

Figure 6 shows the losses as a function of the pitch length for  $N=16$  and  $I/I_c=0.7$ . It can be observed that as the pitch length decreases from 1 m the AC losses first decrease slowly, then more rapidly, when the tape-to-tape gaps tend to close more rapidly.

From the discussion carried out so far one can expect less current penetration inside the tapes wound with a smaller pitches. This is confirmed by figure 7, which shows (always for the case  $N=16$  and  $I/I_c=0.7$ ) the current density distribution (normalized to  $J_c$ ) along the tape's width for different pitch lengths. Also current in twisted tapes tends to be more uniformly distributed inside the tapes and maximum of current density at the sides of the tapes decrease as the pitch decreases.

Figure 8 shows the AC losses as a function of the normalized transport current for three different pitch lengths. The figure extends the results mentioned above to different values of the transport currents. In addition, it can be observed that twisted tapes can transport higher current with lower losses than straight tapes. For example, the AC loss of a twisted tape with pitch length equal to 0.11 m at  $I/I_c=0.9$  is still smaller than the loss in a straight tape at  $I/I_c=0.5$ .

## 5. Conclusion

A new numerical technique to solve the electromagnetic problem of a single-layer coaxial assembly of twisted thin conductors was presented in this paper. The non-linear resistivity of HTS materials can be easily inserted and it can be used to compute the electrical performance of a single-layer HTS cable made of YBCO twisted tapes. After having been tested against a FEM model for straight tapes, the proposed method was applied to find the current density distribution and the AC losses of single-layer HTS cable with different twist pitch length. Among the simulation results it was observed that, for a fixed former radius and a given number of tapes, tapes twisted with smaller pitches shows lower AC losses per cable length unit. This happens in spite of the longer effective length of the superconductor, because the suppression of the perpendicular field component caused by packing the tapes more closely is the dominant effect. The method can be extended to the case of multi-layer cables. This extension as well as the verification of the results with 3D FEM and experimental results will be the subject of a forthcoming publication.

## References

- [1] Nakahata M and Amemiya N 2008 *Supercond. Sci. Techn.* **21** 015007
- [2] Jiang Z, Amemiya N, and Nakahata M 2008 *Supercond. Sci. Techn.* **21** 025013
- [3] Fukui S *et al* 2006 *IEEE Trans. Appl. Supercond.* **16** 143-146
- [4] Fukui S *et al* 2009 *IEEE Trans. Appl. Supercond.* **19** 1714-1717
- [5] Honjo S *et al* 2003 *IEEE Trans. Appl. Supercond.* **13** 1894-1897
- [6] Fukui S *et al* 2006 *IEEE Trans. Appl. Supercond.* **16** 135-138
- [7] Sirois F and Roy F 2007 *IEEE Trans. Appl. Supercond.* **17** 3836-45
- [8] Sirois F, Roy F, and Dutoit B 2009 *IEEE Trans. Appl. Supercond.* **19** 3600-3604
- [9] Brambilla R, Grilli F and Martini L 2007 *Supercond. Sci. Techn.* **20** 16-24